Metallogr. Microstruct. Anal. (2016) 5:16–27
DOI 10.1007/s13632-015-0249-6

TECHNICAL ARTICLE

The Dor 2002/2 Shipwreck, Israel: Characterization of Surviving Ironwork

D. Cvikel[1] · **D. Ashkenazi**[2]

Received: 8 September 2015 / Revised: 22 October 2015 / Accepted: 6 November 2015 / Published online: 23 November 2015

Abstract The Dor 2002/2 shipwreck provides evidence of a 15-m-long vessel built to a high standard, and adds essential information to our knowledge of the construction of small vessels that plied the Eastern Mediterranean during the late Ottoman period. During the underwater excavations of the shipwreck, two metal objects were retrieved: a wooden heart (rigging element) with an iron ring-bolt, and a broken iron chain link with a piece of metal cable. This study aims to understand the manufacturing processes of the objects, and to propose their possible dating. The artifacts were studied by archaeometallurgical testing methods, including, HH-XRF, metallographic stereo, light and SEM–EDS microscopy, and microhardness tests. The results revealed that the ring-bolt was made of ferrite phase with preferred oriented slag inclusions microstructure, as typical for indirect smelted wrought-iron. The chain link was made of gray cast-iron. The suggested date of the shipwreck was 1800; however, based on the archaeometallurgical test results, it is suggested that the two iron artifacts were manufactured between the years 1839 and 1856. This research demonstrates the important contribution of the study of metal finds to the dating of shipwrecks.

Keywords Archaeometallurgy · Cast-iron · Dor 2002/2 shipwreck · Forge-welding · Metallography · Microstructure · Wrought-iron

Introduction

The Dor (Tantura) lagoon is located a few hundred meters south of ancient Tel Dor on the Mediterranean coast of Israel, 30 km south of Haifa (Fig. 1). It is a shallow anchorage, partially protected by four small islands, and can be used in up to maximum Beaufort 4 sea conditions. A navigational channel, through which a south-setting current flows, cuts the lagoon. The prevailing winds during the day are from the south-west in the morning, west about midday, and north-west during the afternoon. At night there is a light easterly breeze. Maneuvring inside the lagoon is tricky, even with local knowledge [1, p. 169].

The advantages, as well as the dangers, of the lagoon were apparent. In 1799, during Napoleon Bonaparte's expedition to the Holy Land, Tantura was chosen for landing supplies, equipment, ammunition, and cannon, and as a communication and evacuation post for the French army besieging Akko [2, pp. 204–206]. Lambert, commander of the Haifa squadron, investigated the anchorage at Tantura. According to his report, the anchorage was suitable for boats and various vessels, but only in fair weather, for in a heavy sea they might run aground or crush against the rocks [3].

Evidence of about 25 shipwrecks has been found in the lagoon. Some have not been excavated, some consist of only a few surviving finds, and 10 have been thoroughly excavated. Shipwreck timbers have been dated to the Roman (37 BC–324 AD), Byzantine (324–638 AD), early Islamic (638–1099 AD), and late Ottoman (1516–1917 AD) periods [1, pp. 169–172]. One of the Ottoman period shipwrecks is Dor 2002/2.

✉ D. Ashkenazi
dana@eng.tau.ac.il

[1] Leon Recanati Institute for Maritime Studies, University of Haifa, Haifa 3498838, Israel

[2] School of Mechanical Engineering, Tel Aviv University, Ramat Aviv 6997801, Israel

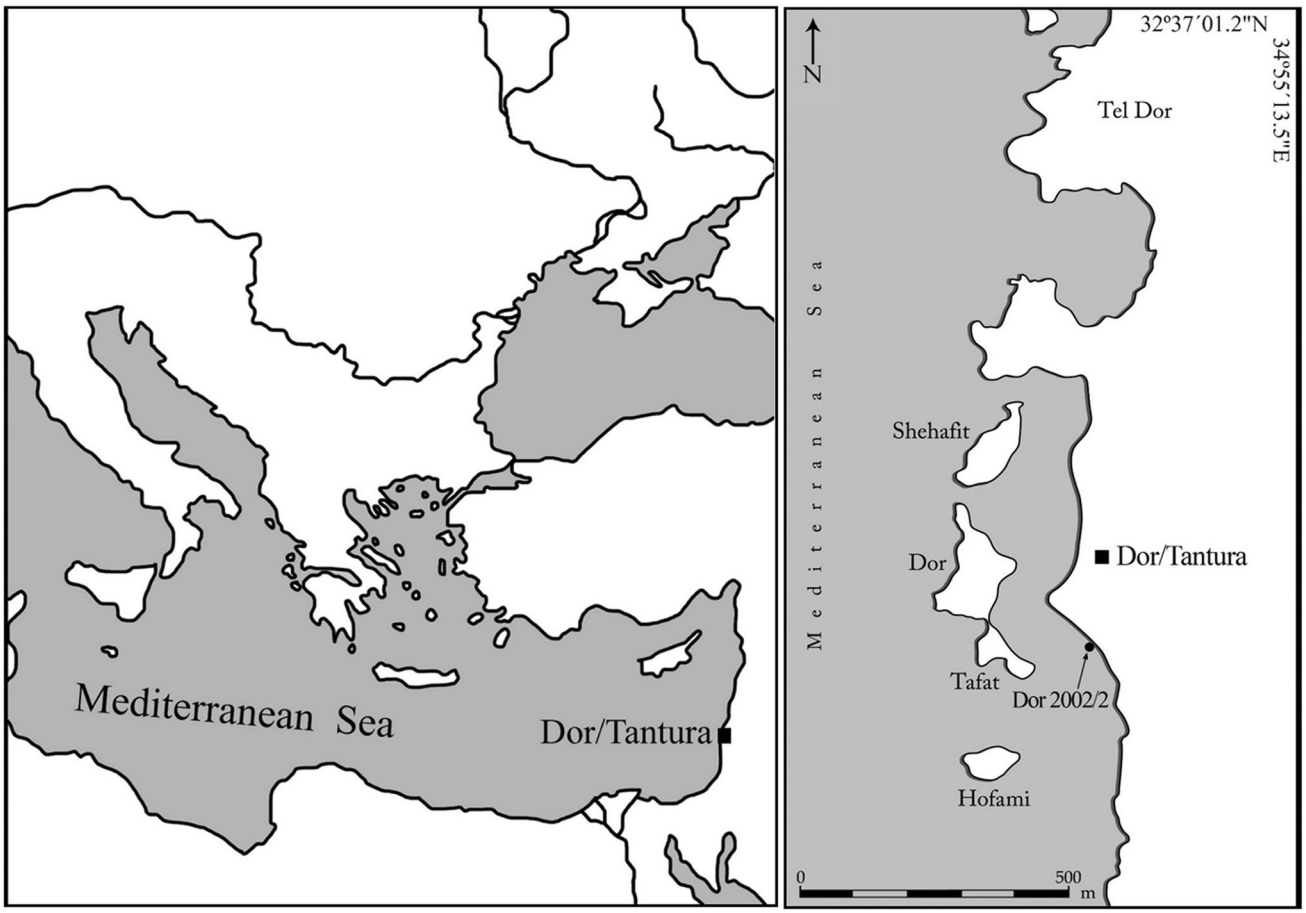

Fig. 1 Location of Dor (Tantura) lagoon and the Dor 2002/2 shipwreck (Drawing: S. Haad)

Dor 2002/2 Shipwreck

The Dor 2002/2 shipwreck was found a few meters from the shore line covered by sand and seashells, and excavated for two seasons (2002, 2003) by the Leon Recanati Institute for Maritime Studies at the University of Haifa. The remains extended 4.7 m from north to south and 5 m from east to west (Fig. 2). The maximum depth of the shipwreck was 1.5 m, with waves washing the excavation site, which was also influenced by the 30 cm tide. Dredgers could be installed and operated only with difficulty, and even the smallest waves hampered the work of the divers [2, pp. 206–207; 4, p. 79; 5, p. 180].

The remains comprised two sections touching each other: the bow area, and a section of the starboard side of the hull of the vessel, and included bow timbers, rising wood, framing timbers, hull planks, a wale, deck beams, and a hawse hole. The hull was built of *Pinus brutia* and *Pinus nigra*, apart from the stem and the treenails, which were made of *Quercus coccifera*. The timbers were carefully worked and shaped, and traces of tool marks were evident, mainly those of an adze and a saw. It has been suggested that the ship was a small, high-quality, fast sailing vessel built in an established Aegean shipyard in Greek tradition. The high standard of the carpentry details indicate a government or military vessel. The ship probably had one mast, and was 15 m long, with a 4.5 m beam and a 1.35 m draught, and had a displacement of about 35 tons [2, pp. 206–211, 214–215; 4; 5, pp. 180–182; for a full description of the Dor 2002/2 shipwreck see Refs. 2 and 4].

Typological dating of the Dor 2002/2 shipwreck was not easy. The best approximate ^{14}C value for the shipwreck is 216 ± 14 years BP. Additional information regarding the age of the shipwreck was obtained by comparison with another shipwreck from Dor—Dor Wreck 2 (DW2), since the ^{14}C dates of the two shipwrecks are similar. Preliminary analysis of the metal finds estimated them to be 200–300 years old [2, pp. 211–213]. Therefore, a date of 1800 was proposed, and it has been suggested that Dor 2002/2 was one of the local craft which were used by the French army stationed in Tantura in 1799 [5, p. 182].

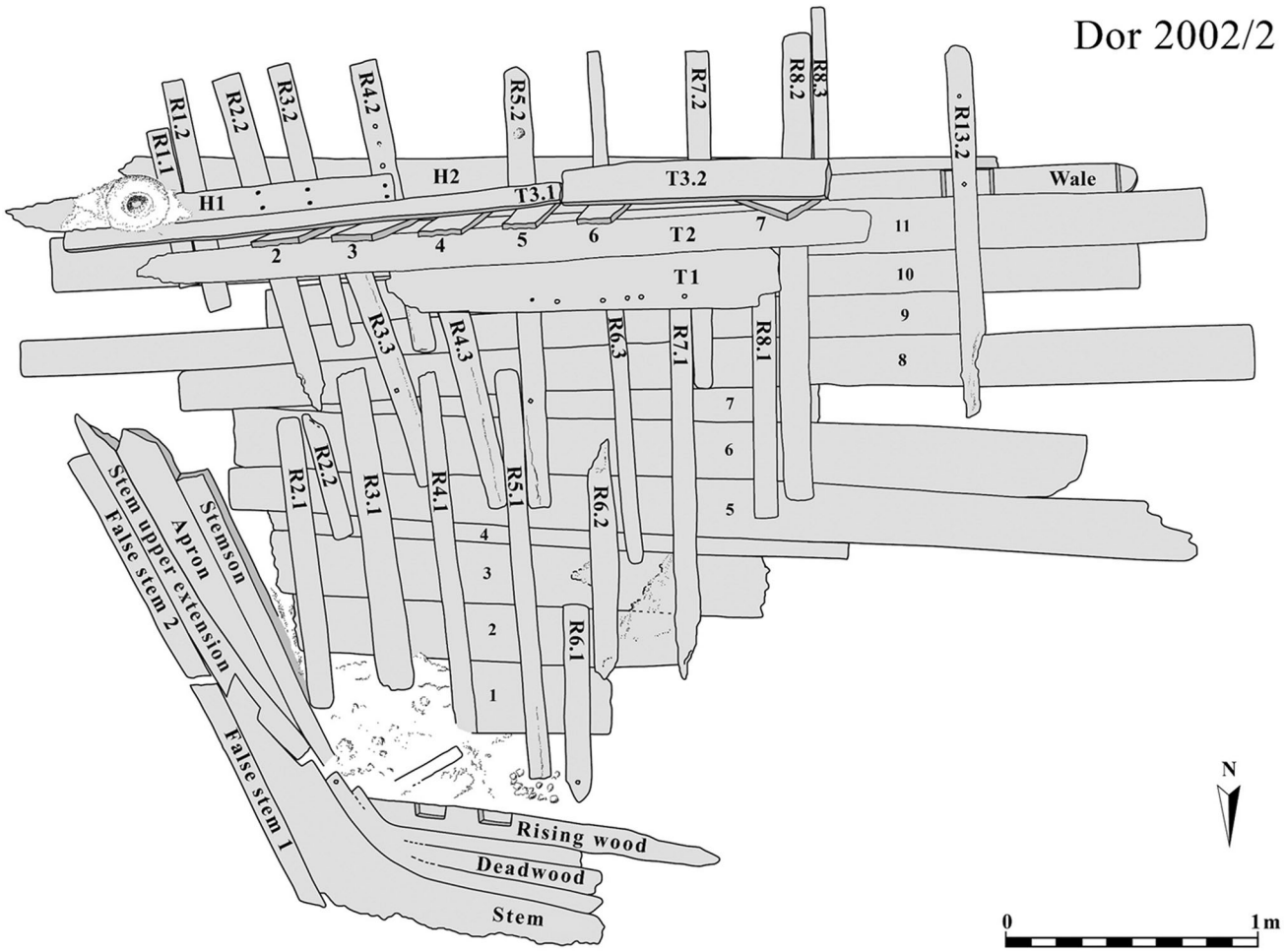

Fig. 2 The Dor 2002/2 shipwreck (Drawing: C. Brandon, adapted by D. Cvikel and S. Haad)

Surviving Ironwork

The heart and ring-bolt were found in situ, covered with encrustation coating and concretion:

1. Item number 101 – a rigging element which was found under the shipwreck (Fig. 3). This was a heart, a rigging element used for setting up the stays of a square-rigged ship. A heart was a triangular or heart-shaped block of wood with a single large hole in the middle, and four to five scores at the bottom, grooved for the lanyard. Around the outside of the heart, a groove for the stay was cut [6, p. 17; 7, p. 381; 8, p. 14; 9, p. 169; 10, p. 251].
   The heart is made of hardwood—*Fagus orientalis* (Oriental beech). The hole dimensions are 3 cm by 4 cm, and three scores and rope-marks are clearly evident. After careful removal of the coating layer, a ring-bolt was exposed in a medium state of preservation, and was strongly attracted to a magnet so that the attraction could be felt.
2. Item number 123 – a broken chain link with a piece of metal cable (Fig. 4) which was found concreted to the hawsehole—a hole in the bow of a ship through which the anchor cable passes [7, p. 380]. Ropes or chains rather than cables are used for anchoring, and therefore, it is possible that the metal cable was used for securing the anchor chain. The piece was 2.3 cm long and 16 mm in diameter when found. However, it was corroded and in a poor state of preservation, and consequently not studied in this research. The broken chain link, however, was strongly attracted to a magnet so that the attraction could be felt.
   In recent years, much experience and knowledge concerning the dating of metal artifact was acquired [e.g., 11–14]. Therefore, it was decided to try and further establish the dating of Dor 2002/2 shipwreck using archaeometallurgical characterization of the two metal artifacts.

Fig. 3 The rigging element as retrieved from the wreck-site (Photo: N. Sheizaf)

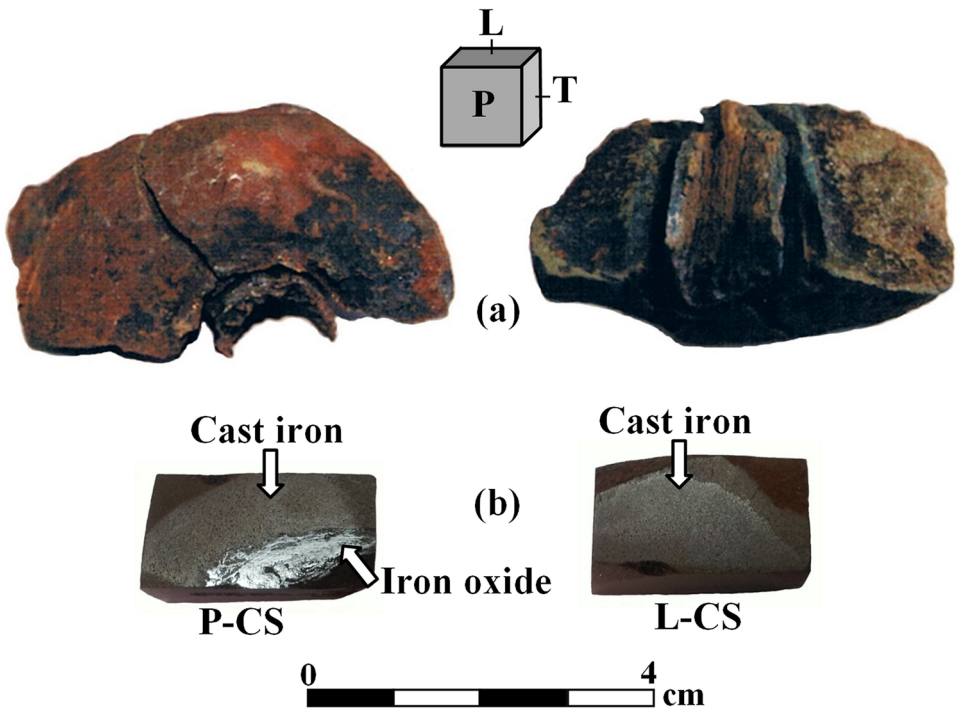

Fig. 4 The broken chain link with remains of a metal cable: (**a**) after removal of the encrustation and concretion coating (Photo: G. Neumann); and (**b**) after grinding and polishing the chain link (Photo: D. Ashkenazi)

Metallurgical Background

Two common technologies were used to produce wrought-iron until the middle of the 19th century: the direct and the indirect smelting methods [14, p. 265; 15, p. 73]. The first smelting method was direct (single stage) smelting, which was performed in a reducing atmosphere below the melting point of pure iron (1538 °C). Inside the furnace, the iron ore reacted with the fuel to form a porous sponge material called 'bloom' [16, p. 1049; 17, pp. 219–221].

During the direct smelting, haematite (Fe_2O_3) was reduced to magnetite (Fe_3O_4), which was then reduced to wüstite (FeO), and at the last stage of smelting was reduced to metallic iron [16, pp. 1049–1050; 17, pp. 219–221; 18, pp. 1745–1757].

The rich slag ore was removed from the solid-state metal as a melt [15, p. 73]. In order to achieve high-quality wrought-iron, a quality haematite ore was used [16, p. 1049]. Since the sponge bloom iron contained a large amount of slag inclusions, additional hot-forging was needed, resulting in a denser and further workable iron ingot [17, p. 221]. At the end of this process a heterogeneous, easily worked and welded wrought-iron was achieved that usually contained an average of 0.1 wt% carbon concentration [17, p. 221; 19, p. 48]. Since silicon, manganese, and phosphorus oxides could not be reduced to their metal state at the low temperatures of the direct smelting process, wrought-iron objects were quite pure [17, pp. 220–221; 20, p. 87]. The ordinary wrought-iron material contained preferentially oriented slag inclusions. The path of the elongated inclusions indicates the plastic-work deformation direction that was used in order to shape a wrought-iron object [21, p. 195].

The second smelting method was indirect. In 1784 the English ironmaster Henry Cort developed a process called 'puddling' to refine pig-iron and convert it into workable wrought-iron, in which pig iron was an intermediate iron product produced from iron ore in a blast furnace. In this indirect process, the molten pig-iron was stirred in a reverberatory furnace in an oxidizing environment, exposing the metal to a high temperature, so that the carbon could be oxidized. As the amount of carbon decreased, the melting temperature of the alloy increased, causing the formation of small semi-solid pieces of iron in the molten material. Next the 'puddler' gathered these pieces of iron and forge-hammered them into iron bars and sheets [19, pp. 128–129, 146, 166]. This technology of refining cast-iron into wrought-iron was used until the middle of the 19th century, but not long after 1856, when the Bessemer process was introduced [17, pp. 221–222; 22, p. 17; 23, p. 156].

Wrought-iron objects were manufactured by solid-state forge-welding joining and, subsequently, were hot-forged to their final desired shape. The forge-welding process is done by applying mechanical loading (hammering) combined with heat treatment [19, p. 48; 24, p. 7]. The welding zone between two wrought-iron parts is characterized by an elevated quantity of non-metallic inclusions; yet the trapped oxides between the welded parts form a rather continuous interfacial [15, pp. 73–74; 25, p. 15; 26, p. 1052; 27, pp. 92–93]. The iron silicate inclusions inside wrought-iron products are residues of the smelting process, but may also have been added during the forge-welding process as sand flux in order to improve the quality of the welding [28, pp. 895–896].

Cast-iron, which is made by a different manufacturing process than the smelting methods of wrought-iron, is a ferrous alloy that contains more than 2 wt% carbon, as well as more than 0.5 wt% silicon. Other typical elements common to cast-iron are sulfur, phosphorus, and manganese [29, p. 38]. Cast-iron alloys are usually classified according to their amount of silicon: white cast-iron contains less than 1 wt% silicon, while gray cast-iron contains more than 1 wt% silicon. As a graphite stabilizer, silicon causes carbon to precipitate as dark graphite flakes, surrounded by a bright ferrite and/or pearlite matrix [30, pp. 9–10; 31, p. 326]. A high concentration of manganese (>0.1 wt% Mn) indicates that the object was manufactured after 1839, when the English metallurgist Josiah Heath registered a patent for the addition of manganese to cast-iron in order to reduce cast porosity and gas holes [14, p. 265; 32, p. 119]. This technological development can be a valuable *terminus post quem* for a post-1839 manufacturing date [e.g., 13].

Iron artifacts retrieved from shipwrecks buried under layers of sand for a long period are usually found covered with a thick encrustation coating and concretion, and suffer severe corrosion, which is accelerated by the presence of chlorides. Such objects have a tendency to corrode around areas of discontinuity such as slag inclusions [11, p. 173].

Experimental Methods and Testing

Non-destructive Testing (NDT)

The NDT of the ring-bolt (item number 101) and the chain link (item number 123) included the following tests:

(a) Visual testing (VT) to identify visible discontinuities and defects.
(b) Hand Held x-ray fluorescence (HH-XRF) chemical analysis was performed. The tests were carried out with an OXFORD X-MET 7500 HH-XRF, using Silicon Drift Detector and LE operation mode. The detected area was 5 mm in diameter, equipped with

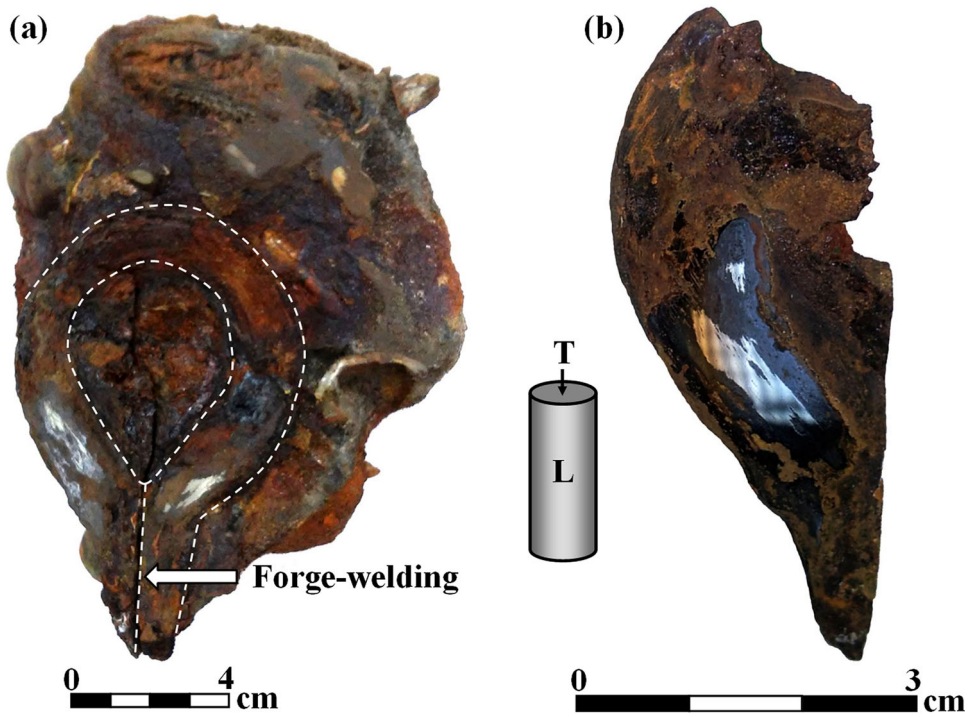

Fig. 5 The ring-bolt: (**a**) the object embedded in the encrustation and concretion coating, showing the forged-welding line (*arrow*); and (**b**) after removal of the coating, showing the iron metal

Table 1 XRF results of the ring-bolt and the chain link

Measured part	Composition (wt%)					
	Fe	P	Si	Mn	S	Ti
Ring-bolt, area 1 (L-CS)	99.8	0.1	…	0.1	…	…
Ring-bolt, area 2 (L-CS)	98.6	0.3	0.9	0.1	0.1	…
Ring-bolt, area 1 (T-CS)	99.8	0.1	…	0.1	…	…
Chain link (P-CS)	90.6	1.2	4.5	3.2	0.1	0.4
Chain link (L-CS)	92.5	0.7	4.7	1.8	0.3	…

a 45 kV Rh target x-ray tube. At each measured area three measurements were performed; 30 s each.

Since HH-XRF is a surface analysis tool, the external surface of the objects may not be representative of their bulk composition [33, pp. 173–174]. In order to avoid such a problem, the samples were sufficiently grinded and polished until their bulk was exposed. Light elements, such as carbon and oxygen, could not be detected with this instrument due to the instrumental limitations.

Destructive Testing

For the metallographic examination of the ring-bolt and the chain link, samples were cut in longitudinal (L-CS), planar (P-CS) and transversal (T-CS) cross sections according to ASTM-E3 standard, and were mounted in Bakelite. The surface was grinded with 120–4000 grit papers, and then polished with 1 μm diamond, and with 0.3 and 0.05 μm alumina pastes. Next, the samples were etched with Nital (97% alcohol and 3% HNO_3) for 40 s.

The testing included:

(a) Stereo microscope (SM) and optical light microscope (LM) examinations.
(b) Environmental scanning electron microscope (ESEM) in high vacuum and an Everhart-Thonley secondary electron (SE) detector. The composition was analyzed by EDS using a Si(Li) liquid-cooled x-ray detector.
(c) Vickers microhardness measurements with microindentation tester using 25 gram-force (gf) load for the iron and 50 gf for the iron-oxide; and a dwell time of 15 s, using ASTM E 384-99 standard for microindentation hardness. The microhardness is given by the average value of five indentations.

Results

The ring-bolt and the chain link were covered with encrustation and concretion. Under their concretion layers, both objects suffered from corrosion, but beneath the external surface the metal survived. Magnetic testing and chemical analysis (XRF and SEM–EDS) of the two artifacts revealed that they were made of iron.

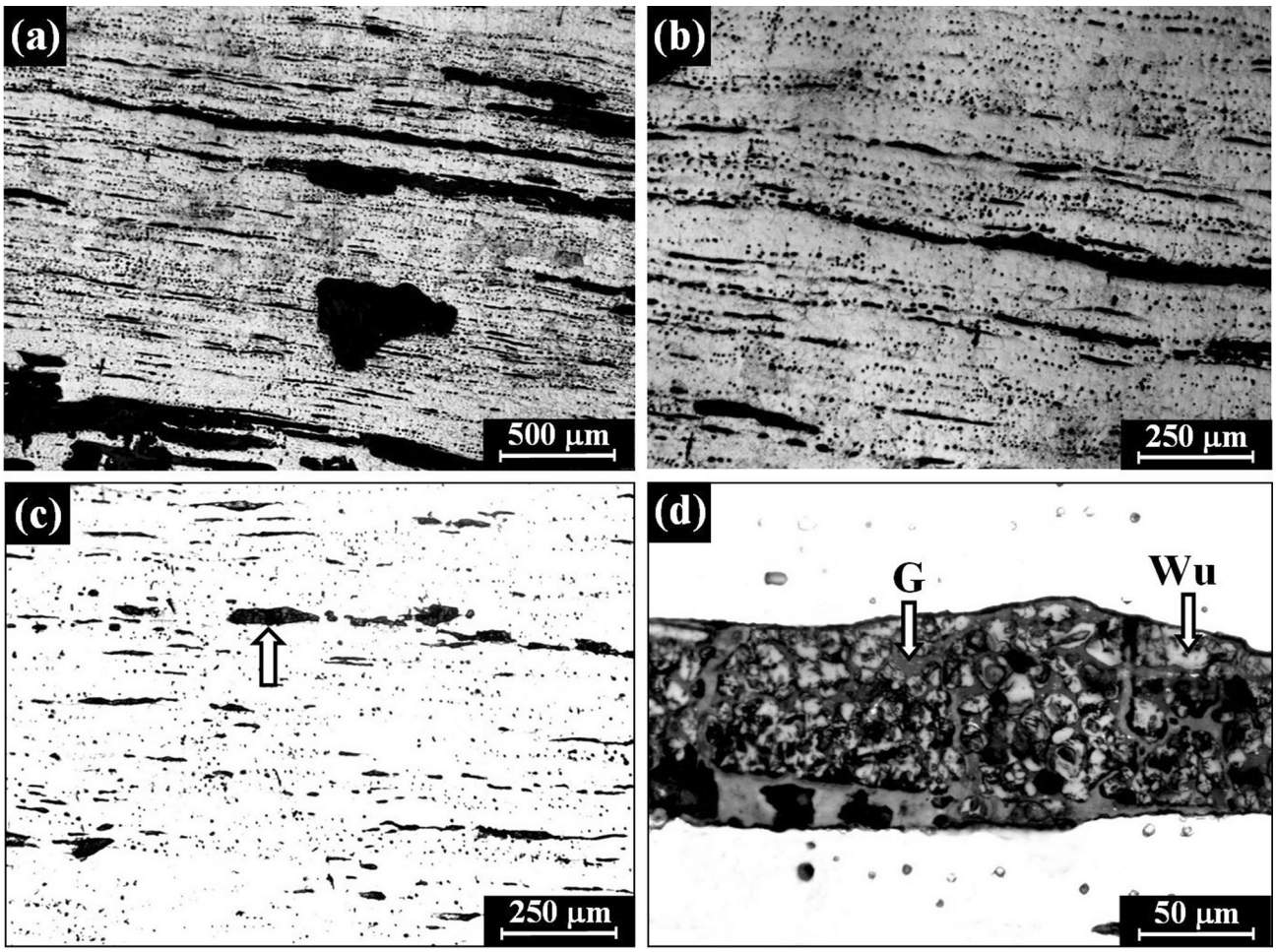

Fig. 6 LM images of the ring-bolt (L-CS): (**a**) holes, cracks and large quantities of slag inclusions surrounded by iron matrix (×50 magnification); (**b**) preferred oriented inclusions (×100); (**c**) a brighter image of the inclusions (×100); and (**d**) higher magnification (×500) of an oriented two-phase slag inclusion (marked with an *arrow* in (**c**) shows circular islands of wüstite (*Wu*) phase surrounded by a glassy (*G*) phase

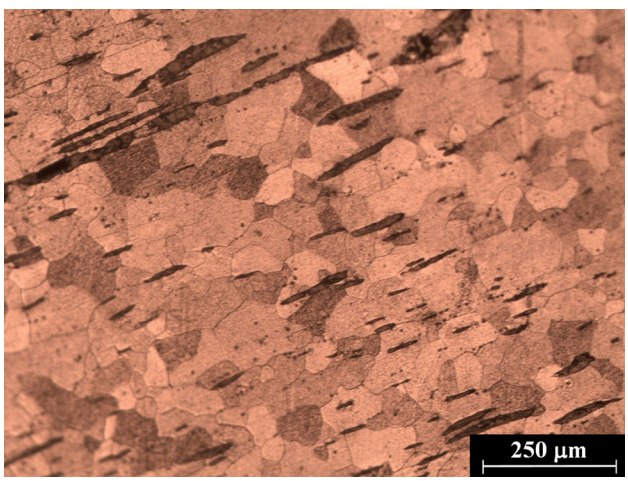

Fig. 7 LM image of the ring-bolt showing large quantities of preferred oriented slag inclusions surrounded by an iron matrix of large equiaxed iron-ferrite grains (L-CS, after etching)

The Ring-Bolt (Item Number 101)

Observation (VT) of the ring-bolt revealed that its loop was forge-welded (Fig. 5, arrow). However, since the area of the forge-welding line was cracked and broken into two parts, and because the welding interface was all corroded, the welding line could not be examined by LM.

XRF analysis of the ring-bolt revealed that it was made of almost pure iron (98.6–99.8 wt% Fe) that also contained 0.1–0.3 wt% P, up to 0.9 wt% Si, 0.1 wt% Mn and up to 0.1 wt% S (Table 1). Metallographic LM of the ring-bolt revealed ferrite matrix, holes, cracks, and large quantities of slag inclusions surrounded by ferrite matrix (Fig. 6). The elongated preferred oriented slag inclusions were parallel to each other (Fig. 6a–c), indicating that the object was made by hot-forging process, and the inclusions were in the direction of the working process. A metallographic LM image of the ring-bolt after etching revealed large

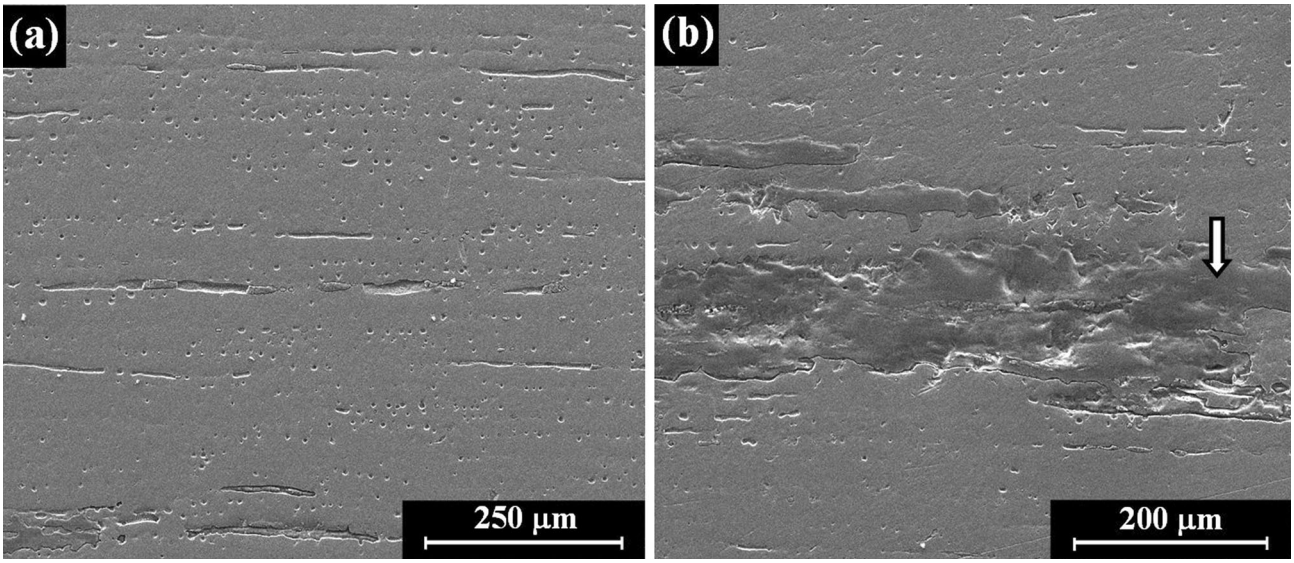

Fig. 8 SEM images of the ring-bolt (L-CS): (**a**) large quantities of preferred oriented slag inclusions surrounded by ferrite matrix; and (**b**) large one-phase slag inclusion (*arrow*) examined by EDS analysis

Table 2 SEM-EDS results (local measurements), using ESEM-FEI Quanta 200FEG from FEI

Measured part	Composition (wt%)									
	Fe	O	P	C	Al	Na	Si	Mn	Cl	Ca
Ring-bolt, iron matrix (L-CS)	99.7	…	0.2	…	…	…	…	0.1	…	…
Ring-bolt (one phase-inclusion, L-CS)	55.9	43.8	…	…	…	…	…	…	…	0.3
Ring-bolt (two-phase inclusion, L-CS)	44.7	35.8	5.2	…	0.6	1.0	5.7	6.2	0.8	…
Chain link (cast-iron matrix, L-CS)	41.4	43.7	4.5	…	…	…	5.7	0.6	4.1	…
Chain link (iron-oxide, L-CS)	51.2	38.0	…	5.8	…	…	…	…	5.0	…
Chain link (graphite flake, L-CS)	…	…	…	100.0	…	…	…	…	…	…

quantities of preferred oriented slag inclusions (10–200 µm long), surrounded by an iron matrix of large equiaxed ferrite grains, 50–180 µm in size, as expected from hot-forged iron (Fig. 7, LM, L-CS).

SEM images of the ring-bolt samples (Fig. 8, L-CS) showed large quantities of parallel preferred oriented slag inclusions surrounded by a ferrite matrix. EDS analysis of the ring-bolt matrix revealed it was made of almost pure iron (99.7 wt%), that also contained 0.2 wt% P and 0.1 wt% Mn (Table 2). Observation of a one-phase large inclusion revealed that it was composed of 55.9 wt% Fe (=26.7 at.% Fe), 43.8 wt% O (=73.0 at.% O), and a small amount of Ca (Fig. 8b—arrow; Table 2). An observation of a two-phase (glass-wüstite) slag inclusion revealed that it was composed of 44.7 wt% Fe (=22.4 at.% Fe), 35.8 wt% O (=61.9 at.% O), 5.2 wt% P (=4.7 at.% P), 5.7 wt% Si (=5.6 at.% Si), and 6.2 wt% Mn (=3.1 at.% Mn), as well as small amounts of Al, Na, and Cl (Table 2).

An observation of the ring-bolt T-CS revealed a ferrite matrix with many equiaxed slag inclusions, but no elongated inclusions, as expected from wrought-iron in the direction perpendicular to the direction of the hot-forging process (Fig. 9, LM).

The average microhardness value of the object's iron matrix was between 190 ± 20 HV (T-CS) and 196 ± 16 HV (L-CS), and the average hardness of the two-phase wüstite-glassy slag inclusion was 386 ± 28 (L-CS) (Table 3).

The Chain Link (Item Number 123)

VT and SM observation of the object's surface revealed the presence of iron-oxide (Fig. 4, arrow). An XRF examination of the chain link revealed a composition of 90.6–92.5 wt% Fe, 0.7–1.2 wt% P, 4.5–4.7 wt% Si, 1.8–3.2 wt% Mn, 0.1–0.3 wt% S, and 0.4 wt% Ti (Table 1). General metallographic SM and LM observation of the link revealed bright and dark areas (Fig. 10). The bright area had an as-cast dendritic structure [13, p. 2524], and active orange-brown corrosion products on the surface,

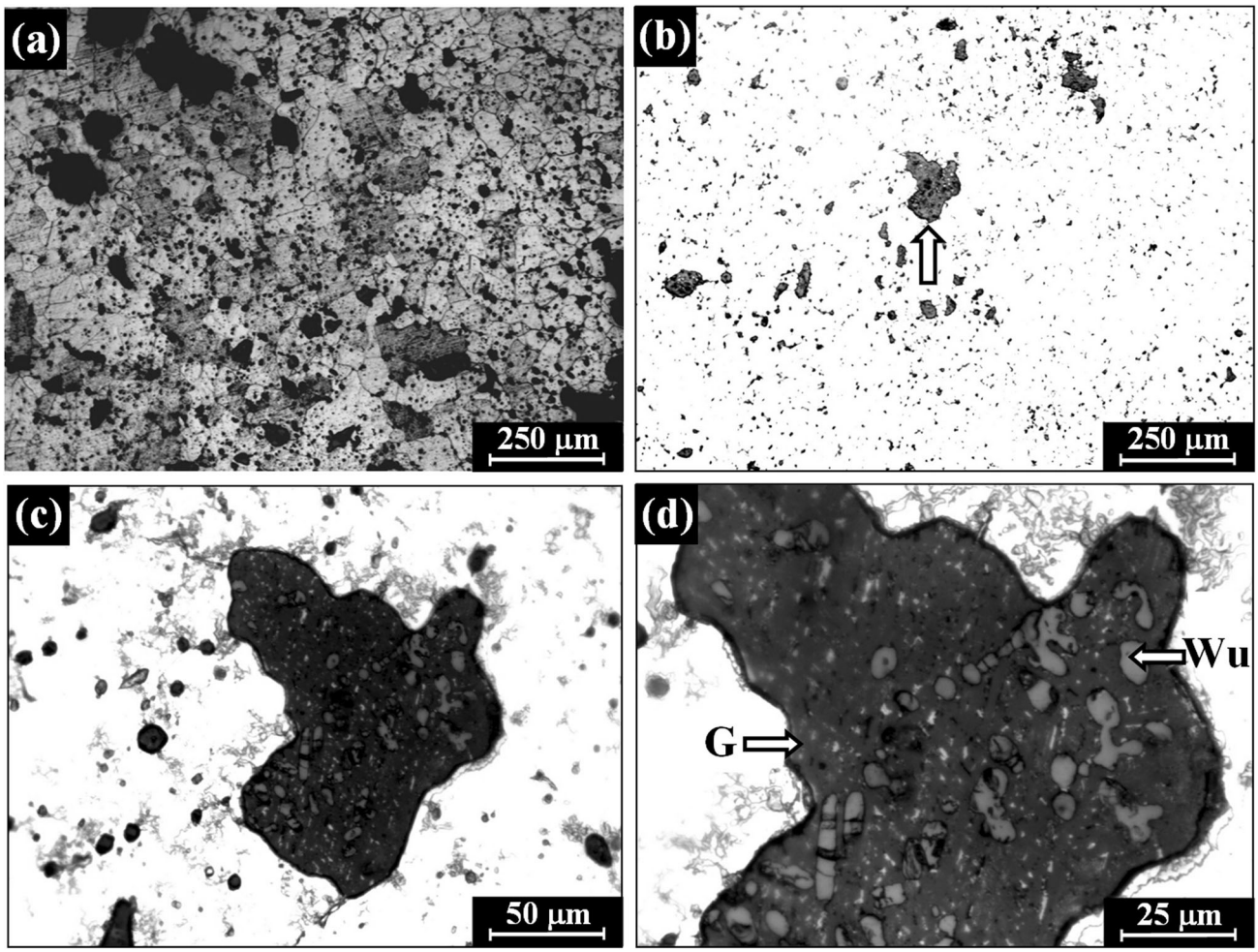

Fig. 9 LM images of the ring-bolt (T-CS): (**a**) ferrite matrix, holes and many slag inclusions (etched); and (**b**)–(**d**) brighter images showing large two-phase slag inclusion of wüstite (*Wu*) phase and a dark glassy (*G*) phase surrounded by iron in different magnifications (up to ×1000)

Table 3 HV microhardness test of the iron artifacts (using 25 gf load)

Sample	Vickers microhardness (HV)			
	Minimum	Maximum	Average	SD
Ring-bolt (iron matrix, T-CS)	164	208	190	20
Ring-bolt (iron matrix, L-CS)	169	209	196	16
Ring-bolt (two-phase inclusions, L-CS)	352	423	386	28
Chain link (dark iron-oxide, P-CS)	287	357	317	26
Chain link (dark iron-oxide, T-CS)	289	369	324	29

as well as porosity, including interdendritic shrinkage porosity formed during solidification.

The dark iron-oxide area revealed many cracks (lower area of Fig. 10a). SEM images of the metallographic link sample revealed that the bright area was made of gray cast-iron with graphite flakes (Fig. 10c). Areas of iron-oxide were also observed (Fig. 10d). SEM higher magnification of the cast revealed graphite flakes surrounded by an iron matrix (ferrite and pearlite); severe porosity occurred according to the environmental corrosion attack of the pearlite (Fig. 11). EDS examination revealed a composition of 41.4 wt% Fe, 43.7 wt% O, 4.5 wt% P, 5.7 wt% Si, 0.6 wt% Mn, and 4.1 wt% Cl (Table 2), as expected from corroded cast-iron. EDS analysis of the dark flakes revealed that they were composed of 100 wt% C. The dark iron-oxide zone revealed a composition of 51.2 wt% Fe, 38.0 wt% O, 5.8 wt% C, and 5.0 wt% Cl (Table 2).

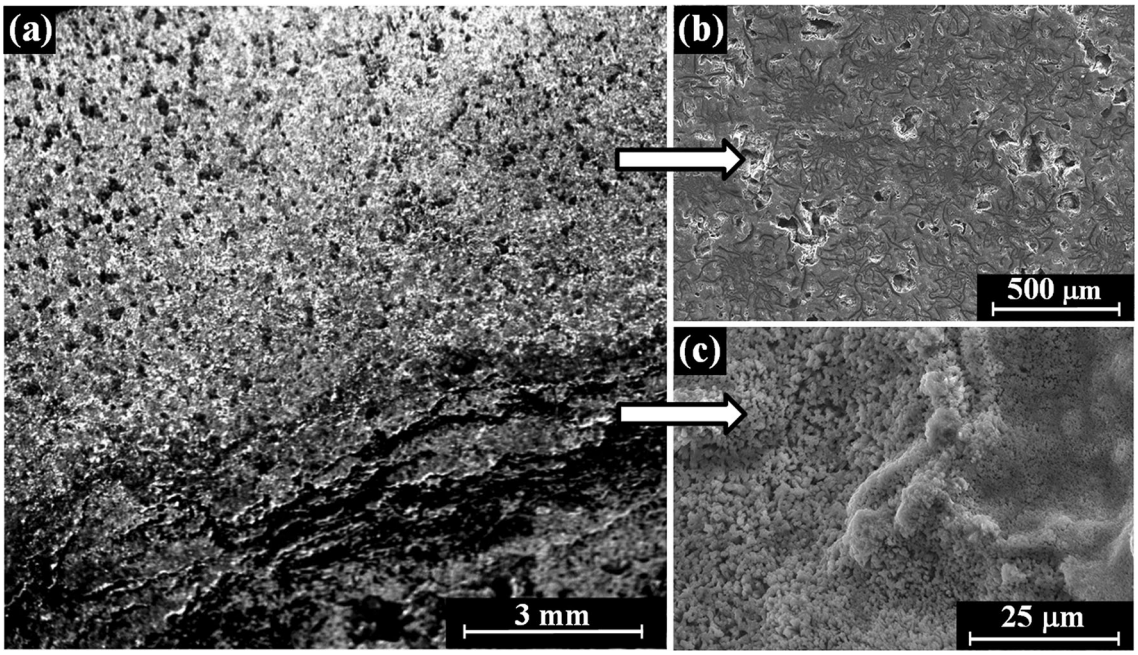

Fig. 10 The chain link: (**a**) cast-iron with porosity and active corrosion (upper area of image), and dark oxide with cracks (lower area of image, SM, P-CS); (**b**) cast-iron with graphite flakes and porosity (SEM, **a**—*upper bright arrow*); and (**c**) iron-oxide (SEM, **a**—*lower bright arrow*)

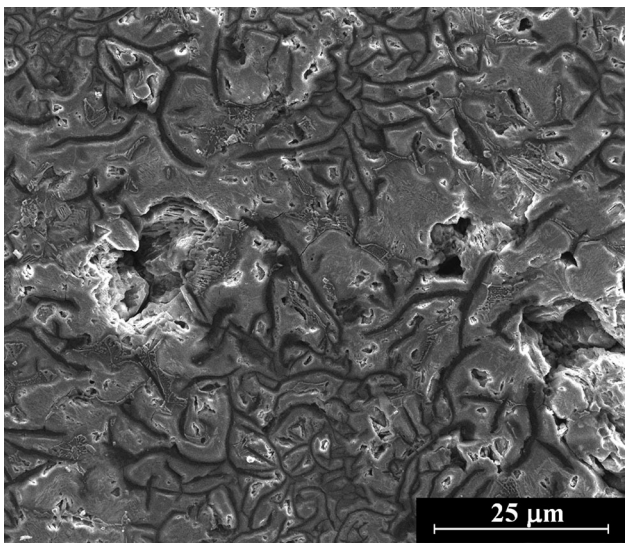

Fig. 11 SEM image of the iron chain link showing gray cast-iron with graphite flakes and severe porosity (P-CS)

Since the brighter areas of the cast-iron had severe porosity and active corrosion, their microhardness values were not measured. The average microhardness value of the dark iron-oxide was between 317 ± 26 HV (P-CS) and 324 ± 29 HV (P-CS) (Table 3). Such results could match microhardness that combined wüstite and magnetite phases [34, p. 275]; however, such oxide microhardness values may also be explained by the presence of cracks in the dark oxide (lower part of Fig. 10a).

Discussion

The evolution of technologies through history, combined with the use of scientific tools, such as analysis of microstructure and chemical characterization, may serve as useful tools to distinguish between manufacturing technologies, and may assist in dating metal objects. The suggested dating of the Dor 2002/2 shipwreck was 1800 [2, pp. 211–213]. The archaeometallurgical analysis of the ring-bolt and chain link retrieved from the shipwreck provides valuable information on their manufacture and dating.

The encrustation around the heart might indicate that it was iron strapped. Iron strapped heart came into use on British warships from 1810 on [9, p. 169]. Although referring to British ships, this information can be used with caution to suggest a post-1810 dating for the heart found in the Dor 2002/2 shipwreck. The ring-bolt was manufactured of rather pure ferrite iron, rich in slag inclusions [glassy (G) and glassy-wüstite (G-Wu)] (Figs. 6–9), where wüstite is a crystalline iron silicate. Based on the homogenous microstructure of the ring-bolt, it was most likely a wrought-iron, produced by the indirect technique of fining pig-iron [15, p. 74; 19, p. 48; 28, p. 896]. The slag inclusions in the ring-bolt were embedded within the ferritic matrix and were elongated in the direction of forging (Fig. 7). The equiaxed iron-ferrite grains combined with preferred oriented slag inclusions (Figs. 6 and 8) indicate that the object was shaped by a hot-forging process [21,

p. 195]. The microhardness results of the ring-bolt, with average values of between 190 ± 20 and 196 ± 16 HV (Table 3), are as expected from a ferrite phase that includes small inclusion particles distributed homogeneously in a wrought-iron ferrite matrix [35, p. 209]. Such microhardness values provide additional support that the object was made of wrought-iron manufactured by indirect fining of pig-iron that was shaped by forge-welding into its final form.

Considering the history of welding and the fact that the ring-bolt was forged-welded, the object was most likely manufactured before 1885 [36; 37, p. 3]. Since the ring-bolt was manufactured by indirect fining of pig-iron into a rather pure wrought-iron, and considering that the 'puddling' process was developed in 1784 to refine pig-iron [19, pp. 128–129, 146, 166; 22, p. 17] the ring-bolt was probably manufactured after 1784, but not long after 1856 [17, pp. 221–222; 22, p. 17; 23, p. 156]. The manganese content in the ring-bolt is 0.1 wt% according to the XRF analysis (Table 1); a level sufficient to suggest an intentional addition of manganese, and a post-1839 manufacturing date [14, p. 265; 32, p. 119]. Thus, a manufacturing date of between 1839 and 1856 is suggested for the ring-bolt.

The chain link was made of gray cast-iron with graphite flakes (Figs. 10c, 11). Both modern gray cast-iron and the metallurgical control of metals were inaugurated at the beginning of the 19th century, between 1810 and 1815 [29, p. 38], which provides a preliminary clue for the manufacturing date of the chain-link. It also contained 1.8–3.2 wt% Mn according to the XRF results (Table 1) and up to 0.6 wt% Mn according to the SEM–EDS local measurements (Table 2). Therefore, similar to the ring-bolt, a post-1839 manufacturing date is suggested for this object [14, p. 265; 32, p. 119].

The suggested date of manufacture of the two iron artifacts—between 1839 and 1856 invalidates the possibility of the ship being one of the local craft which were used by the French army stationed in Tantura in 1799, as previously suggested [5, p. 182]. However, as maneuvring in the lagoon requires skilled handling and local knowledge, it was only entered for a specific purpose such as commerce or fishing. The village consisted of about forty meager houses. Nevertheless, there was a custom-house on site, and a good part of the products of the surrounding country, namely, corn, barley, and cotton, was shipped from the small anchorage of Tantura [38, pp. 90–91; 39, p. 202]. Thus, the Dor 2002/2 shipwreck provides first-hand archaeological evidence and attests to continuous activity in the anchorage during the late Ottoman period. The vessel is high-quality and built to a high standard, indicating a government or military vessel, which could have plied the vicinity of Tantura in order to protect commercial and taxation interests.

Conclusions

The Dor 2002/2 shipwreck is the remains of a 15-m-long, high-quality, fast sailing vessel, built to a high standard. It probably sailed in the vicinity of Tantura in order to protect governmental interests such as commerce and taxation. The archaeometallurgical analysis of the ring-bolt and the chain link indicates manufacturing and dating: the ring-bolt was made of wrought-iron produced by the indirect technique of fining pig-iron, with a quite homogenous microstructure of ferrite phase and preferred oriented slag inclusions, as typical for an annealed product, while the chain link was made of gray cast-iron. Based on the analysis results, it is suggested that the two metal artifacts were manufactured between the years 1839 and 1856. This information refines the dating of the Dor 2002/2 shipwreck, and sheds light on the maritime activity in Dor (Tantura) lagoon in the middle of the 19th century.

Acknowledgments The underwater excavation and research of Dor 2002/2 was partially supported by Lord Jacobs from London, the Israel Science Foundation, the Sir Maurice Hatter Fellowship for Maritime Studies, the Fraenkel Fellowship Committee, the Hecht Trust, and anonymous donors, to whom the authors are grateful. The authors are grateful to Dr. Z. Barkay, the Wolfson Applied Materials Research Centre, Tel Aviv University, and R. Malmazada, Microtech Ltd (Israel), for their valuable assistance. Thanks are due to the licensee for allowing the publication of this work; B. Doron for the English editing; and the anonymous reviewers for their valuable comments.

References

1. Y. Kahanov, Ship reconstruction, documentation, and in situ recording, in *The Oxford Handbook of Maritime Archaeology*, ed. by A. Catambis, B. Ford, D.L. Hamilton (Oxford University Press, Oxford, 2011), pp. 161–181
2. D. Cvikel, Y. Kahanov, H. Goren, E. Boaretto, K. Raveh, Napoleon Bonaparte's adventure in Tantura Lagoon: historical and archaeological evidence. Israel Explor. J. **58**(2), 199–219 (2008)
3. Fonds français 11275. Lettres et pièces diverses relatives à l'expédition d'Egypte. Lambert – fol. 200. Bibliothèque nationale de France, archives et manuscrits.
4. D. Cvikel, Y. Kahanov, The Dor 2002/2 shipwreck. Archaeol. Marit. Mediter. **3**, 79–98 (2006)
5. D. Cvikel, Y. Kahanov, The Ottoman period shipwrecks of Dor (Tantura) lagoon, Israel. Archeol. Postmediev. **18**, 177–188 (2014)
6. G. Biddlecombe, *The Art of Rigging Containing an Explanation of Terms and Phrases, and the Progressive Method of Rigging Expressly Adapted for Sailing Ships* (Charles Wilson, London, 1848)
7. P. Kemp (ed.), *The Oxford Companion to Ships and the Sea* (Oxford University Press, Oxford, 1976)
8. D. Lever, *The Young Sea Officer's Sheet Anchor, or a Key to the Leading of Rigging, and to Practical Seamanship* (John Richardson, London, 1819)

9. J. Lees, *The Masting and Rigging of English Ships of War 1625–1860* (Naval Institute Press, Annapolis, 2007)
10. K.H. Marquardt, *Eighteenth-Century Rig and Rigging* (Conway, London, 2003)
11. D. Ashkenazi, E. Mentovich, Y. Kahanov, D. Cvikel, O. Barkai, A. Aronson, Archaeometallurgical investigation of iron artifacts from shipwrecks: a review, in *Archaeology, New Approaches in Theory and Techniques*, ed. by I. Ollich-Castanyer (InTech Publisher, Rijeka, 2012), pp. 169–186
12. Y. Kahanov, E. Stern, A. Stern, R. Ronen, D. Cvikel, D. Ashkenazi, What ship? Who fired the cannonballs at the wall in Akko? An archaeometallurgical and historical study. Hist. Metall. **46**(2), 98–110 (2012)
13. E.D. Mentovich, D.S. Schreiber, Y. Goren, Y. Kahanov, H. Goren, D. Cvikel, D. Ashkenazi, New insights regarding the Akko 1 shipwreck: a metallurgic and petrographic investigation of the cannonballs. J. Archaeol. Sci. **37**(10), 2520–2528 (2010)
14. M.L. Wayman, Archaeometallurgical contributions to a better understanding of the past. Mater. Charact. **45**(4), 259–267 (2000)
15. V.F. Buchwald, H. Wivel, Slag analysis as a method for the characterization and provenancing of ancient iron objects. Mater. Charact. **40**, 73–96 (1998)
16. M. Cavallini, Thermodynamics applied to iron smelting techniques. Appl. Phys. A **113**(4), 1049–1053 (2013)
17. J.L. Coze, Purification of iron and steels a continuous effort from 2000 BC to AD 2000. Mater. Trans. **41**(1), 219–232 (2000)
18. J. Bénard, A. Michel, J. Philibert, J. Talbot, *Métallurgie Générale* (Masson, Paris, 1984)
19. R.F. Tylecote, *A History of Metallurgy* (The Metals Society, London, 1992)
20. R.F. Tylecote, J.W.B. Black, The effect of hydrogen reduction on the properties of ferrous materials. Stud. Conserv. **25**, 87–96 (1980)
21. N. North, M. Owens, C. Pearson, Thermal stability of cast and wrought marine iron. Stud. Conserv. **21**(4), 192–197 (1976)
22. W.K.V. Gale, The Bessemer steelmaking process. Trans. Newcom. Soc. **46**(1), 17–26 (1973)
23. J.C. Martin, Strands that stands: using wire rope to date and identify archaeological sites. Int. J. Naut. Archaeol. **43**(1), 151–161 (2014)
24. D.A. Scott, *Metallography and Microstructure of Ancient and Historic Metals* (Getty Conservation Institute, Santa Monica, 1991)
25. S. Barella, C. Mapelli, W. Nicodemi, A leap into the beginning of the metal age: recrystallization and carburizing. La Metall. Ital. **4**, 9–16 (2008)
26. C. Mapelli, W. Nicodemi, R.F. Riva, Microstructural investigation of a medieval sword produced in 12th Century AD. ISIJ Int. **47**(7), 1050–1057 (2007)
27. J. Perttula, Wootz Damascus steel of ancient orient. Scand. J. Metall. **33**, 92–97 (2004)
28. J.V.G. Adelantado, M.A.F. Eres, F.M.V. Algarra, J.P. Vicente, F.B. Reig, Analytical study by SEM/EDX and metallographic techniques of materials used in the iron production process during the Iberian period. Talanta **60**, 895–910 (2003)
29. M. Goodway, History of casting, in *ASM Metals Handbook, Vol. 15: Casting*, ed. by H.J. Frissell (ASM International, OH, 1996), pp. 12–54
30. J.S. Park, M.E. Hall, The use of white cast iron in ancient Korea. Inst. Archaeo-Metall. Stud. **25**, 9–13 (2005)
31. W. Xu, M. Ferry, Y. Wang, Influence of alloying elements on as-cast microstructure and strength of gray iron. Mater. Sci. Eng. A **390**, 326–333 (2005)
32. T.S. Wiltzen, M.L. Wayman, Steel files as chronological markers in North American fur trade sites. Archaeometry **41**, 117–135 (1999)
33. A.N. Shugar, Portable X-ray fluorescence and archaeology: limitations of the instrument and suggested methods to achieve desired results, in *Archaeological Chemistry VIII*, ed. by R.A. Armitage, J.H. Burton (American Chemical Society, Washington, DC, 2013), pp. 173–193
34. S. Balos, A. Benscoter, A. Pense, Roman mystery iron blades from Serbia. Mater. Charact. **60**, 271–276 (2009)
35. D. Cvikel, D. Ashkenazi, A. Stern, Y. Kahanov, Archaeometallurgical analysis of a 12-pdr wrought-iron cannonball from the Akko 1 shipwreck, Israel. Mater. Charact. **83**, 198–211 (2013)
36. J.F. Lancaster, The physics of fusion welding. Part 1: The electric arc in welding. Electric power applications. IEE Proc. B **134**(5), 233–254 (1987)
37. R.F. Stanescu, A single pass butt-welded pipe finite element method computer simulation, Unpublished PhD Dissertation, Carleton University, 2005
38. M.E. Rogers, *Domestic Life in Palestine* (Pob and Hitchcock, Cincinnati, 1865)
39. G. Robinson, *Travels in Palestine and Syria Volume I: Palestine* (Henry Colrurn, London, 1837)